

Geochemical studies of Armoor granites, Nizamabad District, Telangana: Evidence of remelting of older crustal source

A.Ajay Kumar^{1*}, Ch. Karunakar¹, M. Srinivas¹, and K. Sreenu¹
¹*Department of Geology, Osmania University, Hyderabad-500007*

Abstract- In order to understand its petrogenesis and involvement in crust formation, we provide petrographic and whole-rock geochemical data for Armoor granitic rocks in the northeastern portion of the Eastern Dharwar Craton (EDC). The coarse-grained, light grey to pinkish color granites of the study area. Plagioclase, quartz, and alkali feldspar comprise the Armoor granite, with biotite displaying altered and intergranular textures. Geochemically, the nature of Armoor granite ranges from metaluminous to peraluminous and magnesian. On the chondrite normalized REE diagram, the Armoor granites have positive europium anomalies; rich Sr/Y, (Dy/Yb) N ratios and reduced Mg[#], Rb/Sr, Rb, Sr indicate that the melting of earlier rocks and residual garnet source formed at high pressures. Furthermore, they comprise greater amounts of LREE than HREE and LILE than HFSE. Nb, Ta, and Ti all display negative anomalies on primitive normalized spider diagrams indicating formed at the subduction zone setting. We hypothesize that the Armoor granites derive from the remelting of earlier rocks.

Keywords: Armoor, Granite, Geochemistry, LREE, LILE, and Remelting.

INTRODUCTION

The northern section of the Eastern Dharwar craton in southern India is composed of granitoids comprising granite gneiss, tonalite-trondhjemite-granodiorite (TTG), and syeno-monzogranites, together with their corresponding microgranular mafic enclaves and dykes [1]–[4]. The age of these basement TTG rocks corresponds to the middle to late Archean and is represented by [5], followed by Archean to Proterozoic granitic events represented by Closepet granite [6]. Due to differing scholarly opinions, the origin of these granitoids remains a topic of debate. These granitoid magmas are mostly linked with collisional or subduction rifting, intraplate, and oceanic settings [7]–[10]. Granitic magmatism comes

from the hydrous melting of the mantle and is the most compelling evidence for Earth's unique subduction zone magmatism [11]. As shown by the Eastern Dharwar Craton, most of the scientists believe that 2.7–2.5 Ga represents the worldwide peak of continental crust expansion [12]. Five lithotypes characterized Archean crust corridor: (i) tonalite–trondhjemite–granodiorite (TTG), evolved mostly during the early phases; (ii) volcano-sedimentary greenstone belt sequences; (iii) late-stage high-K biotite granitic intrusions; (iv) sanukitoids and minor (iv) hybrid granites [8], [13]–[15]. In the Archean, late magmatism of granites was widespread across the world's cratons, and it played a crucial role in the crustal formation, mineralization, tectonic assembly, and cratonic stability [9], [16]. The Eastern Dharwar Craton (EDC) is composed mostly of Neoarchean greenstone, with traces of 3.0 Ga TTG. Through the plume-arc accretion and cratonization processes, the crust formation, reworking, and tectono-magmatic processes of the EDC are described [8], [10].

GEOLOGICAL SETTING

The present Indian subcontinent comprises four major cratons: The Singhbhum craton in the east, the Baster craton in the south-central region, the Aravalli-Bundelkhand craton in the northwest and central areas, and the Dharwar craton in the south (Fig. 1a) [8]. By the end of the Archean epoch, these cratons had achieved stability (2.5 Ga). Throughout peninsular India, various Proterozoic sedimentary basins evolved; the prominent intracratonic Cuddapah basin is situated in the southeastern section of the Dharwar craton. The Dharwar craton (DC) in southern India is the largest Archean cratonic block in peninsular India, occupying a total area of 238,000 km².

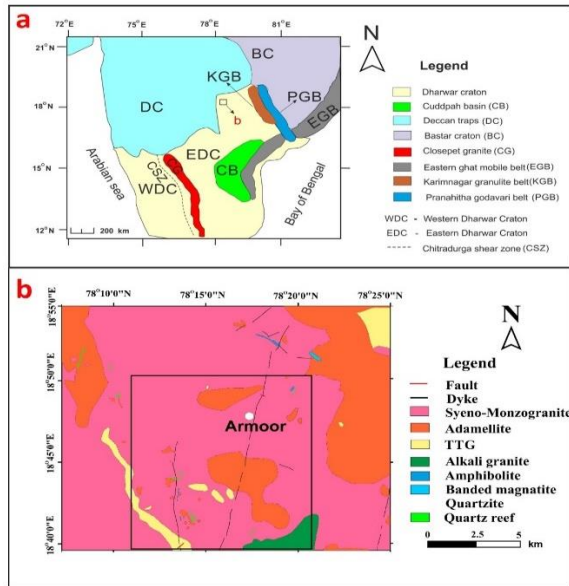


Fig.1 (a) Geological map of the Dharwar craton [21], showing the study area's location. (b) The map illustrates the geology of the Armour area in Telangana, India (modified after the GSI source).

The NW domain of the DC is addressed by the extensive late Cretaceous basaltic flows of the Deccan Traps, whereas the NE region is covered by the Karimnagar Granulite belt (2.6 Ga old); the Eastern part is bounded by the Proterozoic Eastern Ghats Mobile Belt (EGMB), to the south by the Southern Granulite Terrain (SGT) or Pandyan Mobile belt, and to the west by the Arabian Sea. The Narmada–Son lineament delimits the northern boundary of the Dharwar craton [17]. A fault zone trending north-northwest divides the Dharwar craton into the Western Dharwar Craton (WDC) and the Eastern Dharwar Craton (EDC). Before 2.5 Ga, the WDC and EDC had merged [5]. The WDC is made up of TTG-type peninsular gneisses that accumulated in many stages between 3.36 Ga and 3.2 Ga [18], two phases of greenstone belts, the older Sargur Group and the younger Dharwar Supergroup, and calc-alkaline to potassium-rich plutons [19]. Contains TTG gneisses and migmatites with minor 3.38–3.0 Ga crust remnants [20] and many 2.7–2.55 Ga greenstone belt exposures [8], [9].

The Armour Area is situated in the Nizamabad District of the newly established state of Telangana and is dominated by granites emplaced in a Peninsular Gneissic Complex basement complex (Fig. 1b). The Granitic suite of rocks in and around Armour is an integral part of the Archaean Granite complex that

comprises the southern region of Telangana state. The Armour granites' geochemistry is compared to conclude the evolution of the deep continental crust in this area.

FIELD AND PETROGRAPHY

Granitic rocks in the Armour area are generally massive, sometimes foliated, and very rarely gneissic. The Armour granite in the field appears in two colors: grey and pink. The grey granite is more numerous than the pink granite. Several meters of mafic layer percolated in grey granites (Fig. 2a), whereas small mafic layers are associated occasionally (Fig. 2b). The Armour granites are coarse-grained, grey to pink colored, and porphyritic to equigranular in composition. The primary mineral elements of the rocks include orthoclase perthite, microcline, quartz, Plagioclase (oligoclase-andesine), and biotite. The accessory minerals consist of apatite, magnetite, ilmenite, and corundum.

Quartz and alkali feldspar are present in abundance. Under a microscope, granites have dominantly observed crosshatched twining microcline and hosted Plagioclase and quartz crystals, which might influence deformation (Fig.2c). The microstructure of perthite is characterized by the intergrowth of alkali feldspar and plagioclase and surrounded by undulose quartz, which indicate to deformation [22] (Fig. 2d). Plagioclase was strongly sericitized and featured twinned albite polysynthetic structures (Fig. 2e). Rarely, alkali feldspar exhibits sericite alteration and biotite also alter to chlorite (Fig. 2f). Sericitization indicates that the process of alteration has reached low temperatures. Biotite often appears as distinct laths or aggregates transformed into chlorite and epidote.

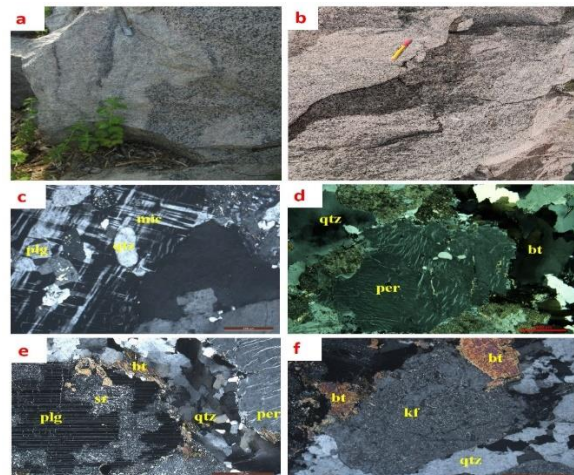


Fig.2 (a) Field photograph depicting the medium-grained grey granite with the mafic minerals. (b) Pink granite shows fine to medium-grain mafic-flow bands. (c) Microcline exhibiting crosshatched twinning with quartz and plagioclase crystals in Armoor granite. (d) coarse-grained perthite hosted quartz crystals and was surrounded by undulose quartz. (e) Plagioclase feldspar display twinning associated seritization and recrystallized quartz crystals. (f) Alkali feldspar and biotite are altered to sericite and chlorite and are surrounded by quartz and feldspar minerals.

ANALYTICAL TECHNIQUES

Granite samples were crushed and powdered using an agate mill and a 200-mesh pulverizer. The "X-Ray Fluorescence Spectrometer (XRF)" at the "CSIR-National Geophysical Research Institute (CSIR-NGRI)" was used to determine the major element concentrations of pressed pellets with a relative standard deviation of 3%; the analytical method is described in "The Journal of Analytical Chemistry" [23]. Using the closed digestion process, materials were dissolved for trace element analysis. In 10 ml Saville containers containing a 7:3 HF: HNO₃ acid combination, 50 mg of representative sample powders were dissolved for 48 hours at 150 °C in a 7:3 HF: HNO₃ acid mixture. After digestion, two to three drops of perchloric acid (HClO₄) were added to the mixture, which was then evaporated until dry. Combining 20 ml of freshly prepared 1:1 HNO₃ and keeping it at 80 degrees Celsius for 10–15 minutes. After getting a clear solution, 5 ml of Rh (1 ppm concentration) was added as an internal standard, and then 250 ml was produced. This solution was diluted to the correct TDS content by adding 5 ml to 50 ml of water (total dissolved solids). Geological Survey of Japan-approved reference materials (JG-2 and JG-1a) were used as standards for the examination of major and trace elements. The reference materials used to determine the accuracy and repeatability of the majority of trace components have an RSD of 5%.

GEOCHEMISTRY

The rocks mostly comprise silica (70.9–72.8 wt %), CaO (0.7–1.31 wt %), and minor quantities of MnO, MgO, and TiO₂. The granites have a moderate total alkali content (9.5–10.1wt%) and a moderate to high

aluminum content (14.1-14.4wt%) (Table 1). The amount of K₂O in granites varies between 5.3 to 6.5%, while the concentration of Na₂O varies between 3.2 to 4.7 wt %. Grey granite has a greater Na₂O/K₂O ratio and CaO concentration than pink granite, which is consistent with the large proportion of K-feldspars in pink granites. A relationship between three factors Ab–Or– An demonstrates an effective categorization of granitoids based on the mineral compositions of sequence with solid solutions, in which the bulk of the analyzed samples are found in the granite field [24] (Fig. 3a). These granites vary from metaluminous to peraluminous nature (Fig. 3b) [25]. The granites had a low Fe[#] value of 0.71-0.79 (Fig. 3c), suggesting the Armoor samples are magnesian in nature [25]. These granites have a higher MALI index, indicating an alkali-calcium composition that is typical of arc rocks (Fig. 3d).

Large ion lithophile elements (LILE), including Ba, Rb, and Sr are more common in the granite samples analyzed than high field strength elements (HFSE) with a greater Sr/Y ratio (Table 2). Chondrite-normalized REE patterns [27] show moderate to high fractionation of LREE/HREE [(La/Yb) N= 16.1-22] and moderate fractionation of LREE/MREE [(La/Sm) N=4.8-7.8] of Armoor granites (Fig. 4a). It has been shown that the fractionation of minerals modifies Eu's chemical behavior. These granites exhibit high positive Eu anomalies (Eu/Eu* = 1.63 to 4.9), as a result of plagioclase fractionation during magma formation [29], [30]. On the Normalized primitive mantle diagram, granites have significant LILE enrichment (Ce, La, U, Rb) and substantial negative P, Nb, and Ti anomalies (Fig. 4b) [28].

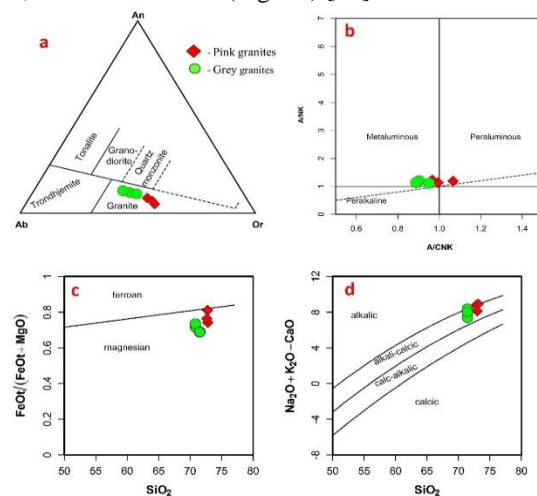


Fig. 3 (a) Ternary diagram An–Ab–Or displaying granite field[26]. (b) Armour granite shows a metaluminous to peraluminous nature in a diagram based on the[25]. (c) $Fe^{\#}$ vs. SiO_2 shows the investigated rocks scatter in the ferroan and magnesian granite fields [25]. (d) SiO_2 vs. MALI-index diagram indicates the alkali-calcic character of Armour granites [25].

DISCUSSION

The Archean–Proterozoic border in the Dharwar Craton is characterized by Neoproterozoic granitic activity, an important event in the processes of crustal formation and melting [31]. Granites may display a wide range of geochemical characteristics based on their origin, degree of melting, and crystallization history [32], [33]. The EDC granites give evidence that younger granites are created by the melting of an older crust (gneisses and TTG) and subsequent fractional crystallisation [16], [34]. The aluminum saturation index [ASI=molar Al/(Ca+Na+K)] of Armour rocks is indicative of the meta-aluminous to per-aluminous nature of melts formed by partial melting of continental crustal rocks, as evidenced by the Th/U (3.1–12.5) and Zr/Hf ratios (28.4–56.8) [35]. Granites are situated inside the remelting of arc crust field in a source discrimination diagram (Fig. 5a), showing that they are derived from older crustal rocks.

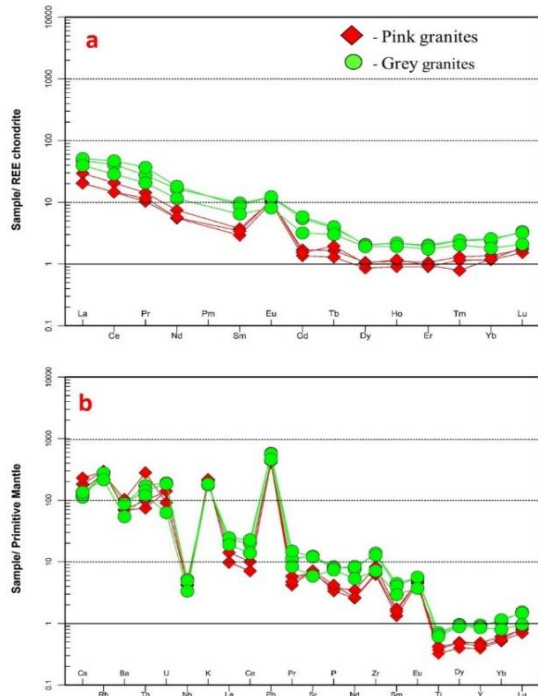


Fig. 4 (a) Chondrite normalized REE patterns of Armour granites exhibit LREE enrichment and HREE depletion[27]. (b) Primitive mantle normalized trace element distribution pattern of Armour granite [28]. Due to the early separation of magnetite and amphibole (garnet) and the suppression of plagioclase fractionation in high pH_2O and fO_2 environments, chronically high Sr/Y ratios (31.8-84.2) and calc-alkaline tendencies are seen [37]. Numerous studies have shown that garnet and amphibole, as remnants of parent rocks, exhibit considerable Sr/Y and La/Yb dissolution [36], [38]. Amphibole, with a partition coefficient K_d for MREE greater than one, consolidates MREE more than HREE, while garnet consolidates HREE more than MREE [30]. In melting, garnet-rich residues would have a higher Dy/Yb ratio than amphibole-rich residues [15], [29], [30]. The Armour granites have positive europium anomalies with LREE enriched, and HREE deficient patterns in conjunction with a greater ratio of Sr/Y (Fig. 5b) [36] and $(Dy/Yb)_N$; these features all suggest to a higher melting pressure of TTG and a metasediment source with garnet residue. In this study, it was revealed that granites with greater Sr/Y, $Mg^{\#}$, and Ni, Eu, LREE, depleted HREE, and decreased Rb/Sr ratios originated from earlier crustal sources.

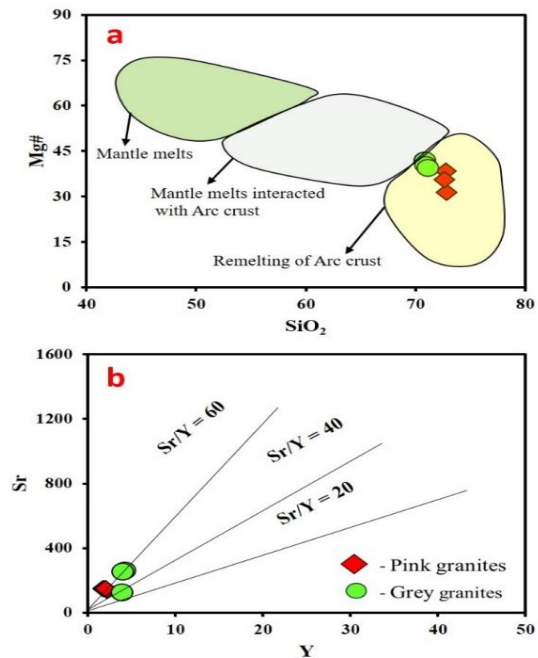


Fig. 5 (a) Source discrimination diagram [with parameters SiO_2 vs. $Mg^{\#}$] the Armour granite falls in the Crustal source [9] and (b) Sr versus Y plot for Armour granites [36].

TECTONIC SETTING

Based on their calc-alkaline composition, magnesian character, and other geochemical indicators, the Armoor granite rocks originated during the last evolutionary phase of the Archean period. Their metaluminous to peraluminous nature and trace element geochemistry prevent their production in volcanic arc and collision situations [25], [39]. Based on the normalized trace element distribution map of the mantle, negative Ba, Sr, Nb, and Ti anomalies imply a subduction zone setting (Fig. 4b). In addition, the HFSE systematics of these granites imply that they are syn-collisional and of volcanic arc type in a subduction context (Fig. 6) [40]. Subduction and collisional orogeny may have thus led to the creation of the Armoor granites in the EDC.

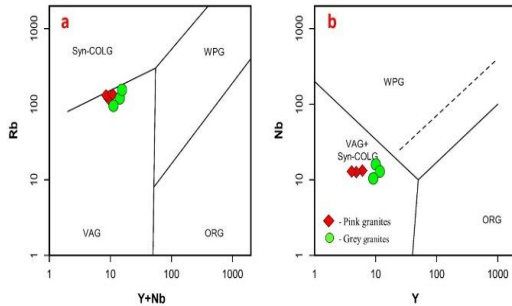


Fig. 6 Armoor granites fall in syn-collisional and volcanic arc settings of the Tectonic discrimination diagram [40].

Table 1. Major oxides (wt%) of Armoor granites from northern part of Eastern Dharwar Craton, Telangana.

Analyte	Pink granites			Grey granites		
	NPT-1	AMR-39	AMR-31	AMR-43	AMR-55	AMR-56
SiO ₂	72.86	72.78	72.63	70.90	70.98	71.15
Al ₂ O ₃	14.48	14.34	14.26	14.20	14.25	14.13
Fe ₂ O ₃	0.79	0.53	0.63	1.13	1.14	1.15
MnO	0.01	0.01	0.01	0.02	0.02	0.02
MgO	0.18	0.17	0.18	0.41	0.39	0.38
CaO	0.76	0.97	0.97	1.26	1.39	1.22
Na ₂ O	3.27	3.46	3.32	4.60	4.78	4.59
K ₂ O	6.29	6.45	6.56	5.44	5.35	5.54
TiO ₂	0.08	0.07	0.09	0.15	0.14	0.13
P ₂ O ₅	0.08	0.07	0.09	0.18	0.17	0.16
Total	98.81	98.83	98.72	98.30	98.61	98.47
Mg#	31.28	38.33	35.64	41.77	40.34	39.41
Fe#	0.80	0.74	0.76	0.71	0.72	0.73
Na ₂ O/K ₂ O	0.52	0.54	0.51	0.85	0.89	0.83

Table 2. Trace and REE compositions (ppm) of Armoor granites from northern part of Eastern Dharwar Craton, Telangana.

Analyte	Pink granites			Grey granites		
	NPT-1	AMR-39	AMR-31	AMR-43	AMR-55	AMR-56
Sc	0.66	0.53	0.79	0.98	0.95	0.84
V	10.89	4.79	5.66	7.29	7.39	6.90
Cr	127.55	127.47	128.57	122.11	121.01	141.68
Co	2.27	1.38	1.40	2.27	2.39	1.35
Ni	7.37	4.99	4.97	6.88	7.42	4.91
Cu	2.27	1.15	1.24	1.83	2.06	1.33
Zn	53.66	24.89	25.12	64.53	65.63	29.14
Ga	12.90	14.41	14.46	15.55	15.79	15.75
Rb	170.56	189.62	185.35	172.07	175.89	136.92
Sr	137.41	150.45	150.53	261.21	253.36	123.93
Y	2.20	1.79	1.99	4.29	4.02	3.89
Zr	92.33	69.54	72.63	154.93	144.58	79.92
Nb	5.01	5.95	5.96	7.66	8.52	9.39
Cs	1.16	1.44	1.83	0.88	0.98	1.07
Ba	723.31	481.15	491.25	612.59	610.69	378.39
La	9.71	6.76	6.70	15.64	16.83	13.07
Ce	17.88	12.59	12.68	35.32	40.57	24.63
Pr	1.60	1.15	1.31	3.08	4.13	2.32
Nd	4.69	3.49	3.56	10.40	11.43	7.24
Sm	0.76	0.59	0.70	1.98	1.78	1.31
Eu	0.81	0.75	0.82	0.93	0.95	0.63
Gd	0.47	0.38	0.42	1.51	1.61	0.88
Tb	0.08	0.06	0.09	0.18	0.19	0.14
Dy	0.37	0.29	0.35	0.71	0.69	0.66
Ho	0.08	0.06	0.08	0.15	0.15	0.13
Er	0.24	0.20	0.21	0.46	0.43	0.39
Tm	0.04	0.03	0.02	0.07	0.07	0.06
Yb	0.30	0.26	0.26	0.53	0.57	0.40
Lu	0.06	0.05	0.06	0.11	0.11	0.07
Hf	3.11	2.00	2.12	4.01	5.10	2.48
Ta	0.19	0.65	0.52	0.18	0.19	0.20
Pb	33.99	29.09	30.02	41.21	40.02	32.72
Th	23.80	6.32	8.42	14.69	12.12	10.15
U	1.90	2.96	2.95	4.00	3.89	1.32
Sr/Y	62.38	84.23	75.82	60.88	62.97	31.83
LaN/YbN	21.45	17.54	16.88	19.49	19.85	22.05
LaN/SmN	7.81	7.02	5.92	4.87	5.80	6.14
Eu/Eu*	4.14	4.90	4.66	1.66	1.72	1.79
Dy/YbN	0.77	0.74	0.85	0.85	0.79	1.06
Sum_REE	37.08	26.68	27.29	71.06	79.53	51.93

CONCLUSION

Metaluminous to peraluminous, calcic-alkaline to alkali-calcic, mostly consisting of K-feldspar, Plagioclase, quartz, and biotite. Armoor granites exhibit a relative increase in LREE over HREE, rich (Dy/Yb) and Sr/Y ratios, and negative Ti, Sr, Ti, and Nb anomalies, which suggests the high-pressure melting of source material with garnet residue in a subduction setting. The current study demonstrates that the Armoor granites are generated in a volcanic arc and syn-collisional setting by remelting prior crustal sources in a subduction zone environment. This process seems to have persisted throughout the

Neoproterozoic, culminating in the development of granites and the completion of the cratonization of the Eastern Dharwar Craton.

ACKNOWLEDGMENT

The Head of the Geology Department at Osmania University (Hyderabad) and the CSIR-National Geophysical Research Institute provided the lab facilities (Hyderabad). Ajay Kumar expresses gratitude for the UGC's RGNF-Research Fellowship (New Delhi). Additionally, we would like to thank to M. Sairam, Y.V. Laxminarayana and K. Rajendra Prasad for assisting with fieldwork and petrographic study.

REFERENCE

- [1] B. C. Prabhakar, M. Jayananda, M. Shareef, and T. Kano, "Petrology and geochemistry of late archaean granitoids in the northern part of Eastern Dharwar Craton, Southern India: Implications for transitional geodynamic setting," *J. Geol. Soc. India*, vol. 74, no. 3, pp. 299–317, 2009, doi: 10.1007/s12594-009-0137-2.
- [2] C. Ashok, E. V. S. S. K. Babu, S. Dash, and G. H. N. V. Santhosh, "Redox Condition and Mineralogical Evidence of the Magma Mixing Origin of the Mafic Microgranular Enclaves (MMEs) from Sircilla Granite Pluton (SGP), Eastern Dharwar Craton (EDC), India," *J. Geol. Soc. India*, vol. 98, no. 9, pp. 1237–1243, 2022.
- [3] C. Ashok, G. H. N. V. Santhosh, S. Dash, and J. Ratnakar, "Magma Mixing and Mingling during Pluton Formation: A Case Study through Field, Petrography and Crystal Size Distribution (CSD) Studies on Sircilla Granite Pluton, India," *J. Geol. Soc. India*, vol. 98, no. 6, pp. 815–821, 2022.
- [4] B. V. Raju, A. D. Asokan, R. Pandey, A. G. Panicker, and M. R. Mohan, "Neoproterozoic crust–mantle interactions from the Eastern Dharwar Craton: Insights from mineral chemistry of the Nizamabad granites, southern India," *J. Earth Syst. Sci.*, vol. 131, no. 3, 2022, doi: 10.1007/s12040-022-01903-3.
- [5] B. Chadwick, V. N. Vasudev, and G. V. Hegde, "The Dharwar craton, southern India, interpreted as the result of Late Archaean oblique convergence," *Precambrian Res.*, vol. 99, no. 1–2, pp. 91–111, 2000, doi: 10.1016/S0301-9268(99)00055-8.
- [6] M. Jayananda, H. Martin, J. J. Peucat, and B. Mahabaleswar, "Late Archaean crust–mantle interactions: geochemistry of LREE-enriched mantle derived magmas. Example of the Closepet batholith, southern India," *Contrib. to Mineral. Petrol.*, vol. 119, no. 2–3, pp. 314–329, 1995, doi: 10.1007/BF00307290.
- [7] J. F. Moyen *et al.*, "Collision vs. subduction-related magmatism: Two contrasting ways of granite formation and implications for crustal growth," *Lithos*, vol. 277, pp. 154–177, 2017, doi: 10.1016/j.lithos.2016.09.018.
- [8] M. Jayananda *et al.*, "Multi-stage crustal growth and Neoproterozoic geodynamics in the Eastern Dharwar Craton, southern India," *Gondwana Res.*, vol. 78, pp. 228–260, 2020, doi: 10.1016/j.gr.2019.09.005.
- [9] M. Jayananda, M. Santosh, and K. R. Adhisheshan, "Formation of Archean (3600–2500 Ma) continental crust in the Dharwar Craton, southern India," *Earth-Science Rev.*, vol. 181, pp. 12–42, 2018, doi: 10.1016/j.earscirev.2018.03.013.
- [10] C. Manikyamba and R. Kerrich, "Eastern Dharwar Craton, India: Continental lithosphere growth by accretion of diverse plume and arc terranes," *Geosci. Front.*, vol. 3, no. 3, pp. 225–240, 2012, doi: 10.1016/j.gsf.2011.11.009.
- [11] J. F. Moyen, "The composite Archaean grey gneisses: Petrological significance, and evidence for a non-unique tectonic setting for Archaean crustal growth," *Lithos*, vol. 123, no. 1–4, pp. 21–36, 2011, doi: 10.1016/j.lithos.2010.09.015.
- [12] M. Jayananda *et al.*, "Geochronology and geochemistry of Meso- to Neoproterozoic magmatic epidote-bearing potassic granites, western Dharwar Craton (Bellur–Nagamangala–Pandavpura corridor), southern India: implications for the successive stages of crustal reworking and cratonization," *Geol. Soc. London, Spec. Publ.*, pp. SP489-2018–125, 2019, doi: 10.1144/sp489-2018-125.
- [13] O. Laurent, H. Martin, J. F. Moyen, and R. Doucelance, "The diversity and evolution of late-Archaean granitoids: Evidence for the onset of 'modern-style' plate tectonics between 3.0 and

- 2.5 Ga,” *Lithos*, vol. 205. pp. 208–235, 2014. doi: 10.1016/j.lithos.2014.06.012.
- [14] M. R. Mohan, A. D. Asokan, and S. A. Wilde, “Crustal growth of the Eastern Dharwar Craton: a Neoproterozoic collisional orogeny?,” *Geol. Soc. London, Spec. Publ.*, pp. SP489-2019–108, 2019, doi: 10.1144/sp489-2019-108.
- [15] J. Nagamma, J. Ratnakar, A. Ajay kumar, and A. Ch, “Geochemical studies of hybrid granite from Madugulapalli area, Eastern Dharwar Craton, Southern India: Implications for crustal mixing,” *Acta Geochim.*, 2022, doi: 10.1007/s11631-022-00568-5.
- [16] P. J. Sylvester, “Archean Granite Plutons,” *Dev. Precambrian Geol.*, vol. 11, no. C, pp. 261–314, 1994, doi: 10.1016/S0166-2635(08)70225-1.
- [17] J. J. W. Rogers, “The Dharwar craton and the assembly of Peninsular India,” *J. Geol.*, vol. 94, no. 2, pp. 129–143, 1986, doi: 10.1086/629019.
- [18] J. J. PEUCAT, B. MAHABALESWAR, and M. JAYANANDA, “Age of younger tonalitic magmatism and granulitic metamorphism in the South Indian transition zone (Krishnagiri area); comparison with older Peninsular gneisses from the Gorur–Hassan area,” *J. Metamorph. Geol.*, vol. 11, no. 6, pp. 879–888, 1993, doi: 10.1111/j.1525-1314.1993.tb00197.x.
- [19] M. Jayananda, D. Chardon, J. J. Peucat, and R. Capdevila, “2.61 Ga potassic granites and crustal reworking in the western Dharwar craton, southern India: Tectonic, geochronologic and geochemical constraints,” *Precambrian Res.*, vol. 150, no. 1–2, pp. 1–26, 2006, doi: 10.1016/j.precamres.2006.05.004.
- [20] A. P. Nutman, V. R. McGregor, C. R. L. Friend, V. C. Bennett, and P. D. Kinny, “The Itsaq Gneiss Complex of southern West Greenland; the world’s most extensive record of early crustal evolution (3900–3600 Ma),” *Precambrian Res.*, vol. 78, no. 1–3 SPEC. ISS., pp. 1–39, 1996, doi: 10.1016/0301-9268(95)00066-6.
- [21] J. Nagamma and C. Ashok, “Microstructural studies on the Madugulapalli Granites, Eastern Dharwar Craton, southern India,” vol. 26, no. 2, pp. 144–154, 2022.
- [22] C. Ashok, G. H. N. V. Santhosh, and J. Vijaya Kumar, T Nagamma, “Evolution of quartz crystals in the Sircilla granite pluton, Southern India: Insights from a Cathodoluminescence study,” *J. Indian Geophys. Union*, vol. 25, no. 6, pp. 57–67, 2021.
- [23] A. K. Krishna, N. N. Murthy, and P. K. Govil, “Multielement analysis of soils by wavelength-dispersive X-ray fluorescence spectrometry,” *At. Spectrosc.*, vol. 28, no. 6, pp. 202–214, 2007.
- [24] Barker, “Trondhjemites: definition, environment and hypotheses of origin,” *Dev. Pet.*, vol. 6, pp. 1–12, 1979.
- [25] B. R. Frost, C. G. Barnes, W. J. Collins, R. J. Arculus, D. J. Ellis, and C. D. Frost, “A geochemical classification for granitic rocks,” *J. Petrol.*, vol. 42, no. 11, pp. 2033–2048, 2001, doi: 10.1093/petrology/42.11.2033.
- [26] J. O’Conner, “A classification for quartz-rich igneous rocks based on feldspar ratios,” *U.S. Geol. Surv. Prof. Pap.*, no. 525, pp. 79–84, 1965.
- [27] [27] N. Nakamura, “Determination of REE, Ba, Fe, Mg, Na and K in carbonaceous and ordinary chondrites,” *Geochim. Cosmochim. Acta*, vol. 38, no. 5, pp. 757–775, 1974, doi: 10.1016/0016-7037(74)90149-5.
- [28] S. S. Sun and W. F. McDonough, “Chemical and isotopic systematics of oceanic basalts: Implications for mantle composition and processes,” *Geol. Soc. Spec. Publ.*, vol. 42, no. 1, pp. 313–345, 1989, doi: 10.1144 /GSL.SP.1989.042.01.19.
- [29] C. G. Macpherson, S. T. Dreher, and M. F. Thirlwall, “Adakites without slab melting: High pressure differentiation of island arc magma, Mindanao, the Philippines,” *Earth Planet. Sci. Lett.*, vol. 243, no. 3–4, pp. 581–593, 2006, doi: 10.1016/j.epsl.2005.12.034.
- [30] J. P. Davidson, D. J. Morgan, B. L. A. Charlier, R. Harlou, and J. M. Hora, “Microsampling and isotopic analysis of igneous rocks: Implications for the study of magmatic systems,” *Annu. Rev. Earth Planet. Sci.*, vol. 35, pp. 273–311, 2007, doi: 10.1146/annurev.earth.35.031306.140211.
- [31] M. Jayananda, J. J. Peucat, D. Chardon, B. K. Rao, C. M. Fanning, and F. Corfu, “Neoproterozoic greenstone volcanism and continental growth, Dharwar craton, southern India: Constraints from SIMS U–Pb zircon geochronology and Nd isotopes,” *Precambrian Res.*, vol. 227, pp. 55–76, 2013, doi: 10.1016/j.precamres.2012.05.002.
- [32] D. J. DePaolo, “Trace element and isotopic effects of combined wallrock assimilation and fractional

- crystallization,” *Earth Planet. Sci. Lett.*, vol. 53, no. 2, pp. 189–202, 1981, doi: 10.1016/0012-821X(81)90153-9.
- [33] J. Ray, A. Saha, S. Ganguly, V. Balaram, A. Keshav Krishna, and S. Hazra, “Geochemistry and petrogenesis of Neoproterozoic Myllem granitoids, Meghalaya Plateau, northeastern India,” *J. Earth Syst. Sci.*, vol. 120, no. 3, pp. 459–473, 2011, doi: 10.1007/s12040-011-0084-3.
- [34] A. Pahari, P. Prasanth, D. M. Tiwari, C. Manikyamba, and K. S. V. Subramanyam, “Subduction–collision processes and crustal growth in eastern Dharwar Craton: Evidence from petrochemical studies of Hyderabad granites,” *J. Earth Syst. Sci.*, vol. 129, no. 1, 2020, doi: 10.1007/s12040-019-1296-1.
- [35] A. Kaygusuz, M. Arslan, F. Sipahi, and İ. Temizel, “U–Pb zircon chronology and petrogenesis of Carboniferous plutons in the northern part of the Eastern Pontides, NE Turkey: Constraints for Paleozoic magmatism and geodynamic evolution,” *Gondwana Res.*, vol. 39, pp. 327–346, 2016, doi: 10.1016/j.gr.2016.01.011.
- [36] J. Nandy, S. Dey, and E. Heilimo, “Neoarchean magmatism through arc and lithosphere melting: Evidence from eastern Dharwar Craton,” *Geol. J.*, vol. 54, no. 5, pp. 3148–3166, 2019, doi: 10.1002/gj.3498.
- [37] M. M. Zimmer *et al.*, “The role of water in generating the calc-alkaline trend: New volatile data for aleutian magmas and a new tholeiitic index,” *J. Petrol.*, vol. 51, no. 12, pp. 2411–2444, 2010, doi: 10.1093/petrology/egq062.
- [38] W. K. Lieu and R. J. Stern, “The robustness of Sr/Y and La/Yb as proxies for crust thickness in modern arcs,” *Geosphere*, vol. 15, no. 3, pp. 621–641, 2019, doi: 10.1130/GES01667.1.
- [39] J. D. Clemens, R. W. Belcher, and A. F. M. Kisters, “The Heerenveen batholith, Barberton Mountain Land, South Africa: Mesoarchean, potassic, felsic magmas formed by melting of an ancient subduction complex,” *J. Petrol.*, vol. 51, no. 5, pp. 1099–1120, 2010, doi: 10.1093/petrology/egq014.
- [40] J. A. Pearce, N. B. W. Harris, and A. G. Tindle, “Trace element discrimination diagrams for the tectonic interpretation of granitic rocks,” *J. Petrol.*, vol. 25, no. 4, pp. 956–983, 1984, doi: 10.1093/petrology/25.4.956.